

COMPARISON OF INDOOR CLIMATE IN DETACHED AND MULTI-SPAN GREENHOUSES

S Kruger^{*}, L Pretorius^{}**

^{*}Author for Correspondence, Department of Mechanical Engineering Science,
University of Johannesburg, Kingsway Rd, Auckland Park, Johannesburg, South Africa, E-mail: skruger@uj.ac.za

^{**} Faculty of Engineering , the Built Environment and Information Technology ,Graduate School of
Technology Management , University of Pretoria ,South Africa. E-mail: Leon.Pretorius@up.ac.za

NOMENCLATURE

ρ	[kg/m ³]	Density
Φ	*	Scalar Quantity
V	[m/s]	Velocity
v_g	*	Grid Velocity
Γ	*	Diffusion Coefficient
A	*	Face Area
g	[m/s ²]	Gravitational Vector
G	*	Grid Flux Computed from mesh motion
S_Φ	[-]	Source Term
T_{ref}	[K]	Operating Temperature
β	[/K]	Coefficient of Bulk Expansion
Subscripts and Superscripts		
o	[-]	Cell Number
f	[-]	Face Quantity
V		Cell Volume

* For units refer to the StarCCM+ Documentation [12]

ABSTRACT

The purpose of this paper is to investigate and compare the indoor climate of detached and connected greenhouses. The velocity and temperature distribution inside these greenhouses are numerically analysed using computational fluid dynamics. The initial four span greenhouse was validated in a previous paper [10]. In the first case evaluated, a second greenhouse was placed behind the first greenhouse. Secondly, the first four span greenhouse was extended by adding four additional spans, creating an eight span greenhouse. Lastly, the first case was extended by moving the second greenhouse to the leeward side so as to create a distance of 2m between them. Results showed that by adding an additional four spans, or by attaching four extra spans, the indoor climate inside the greenhouse is influenced to some extent. If the velocity and temperature distributions in the first four and last four spans are compared, a notable difference is found which may influence crop growth.

INTRODUCTION

Ventilation in plant production systems is of vital importance to maintain a healthy indoor climate. Adequate ventilation of greenhouses can assist in the controlling of the indoor temperature, renewing the carbon dioxide supply, and to reduce the relative humidity of the greenhouse. With the recent emphasis on energy conservation, the popularity of natural ventilation as an alternative option to mechanical systems has increased. The ventilation in naturally ventilated greenhouses is driven by pressure differences created at intentional openings, such as roof and side vents. These pressure differences are caused by temperature differences between the inside and the outside of the greenhouse, commonly known as the buoyancy or stack effect, as well as outside wind effect [1]. Multi-span greenhouses are often used in large plant production facilities. Detached greenhouses have certain advantages over multi-span greenhouses. It is claimed that detached greenhouses are easier to ventilate, and that light entering the greenhouse is distributed relatively uniformly [2]. Caring and maintenance are also less tiresome compared to connected structures. Multi-span greenhouses on the other hand need less land area, fewer construction materials are required, and less heat is required as there are less exposed wall surfaces. Unfortunately, the air velocity and indoor climate inside large greenhouses vary considerably, which could interfere with crop growth. [3]

Advances in computer technology of the last decade have made it possible to use Computational Fluid Dynamics (CFD) to investigate the indoor climate of greenhouses. A thorough review on the applications of CFD in the modelling and design of ventilation systems in the agricultural industry was published by [4]. It was found that the quality of the solutions is dependant on the chosen turbulence model. The author concluded that greenhouse investigations have generally been of a higher standard compared to animal housing, since crop biological models have been incorporated in the computational models. The indoor airflow have been investigated by several authors using CFD. [5,6,7] Work done by Shilo et al [3] also refers

to experimental work that may be useful to calibrate future and current CFD studies in future papers. CFD have also been used to investigate the influence of various vents arrangements in greenhouses [6,8,9]. The influence of internal partitions has been studied to some extent in previous work done by this author [10].

Various studies on specifically multi-span greenhouses have been conducted. Lee-side ventilation-induced air movement were experimentally investigated by Wang et al [11] in a large 12 span venlo-type greenhouse. It was concluded that horizontal air velocities at various locations were proportional to the external wind speed and the opening angle. It was also found that the airflow in the horizontal plane was of low turbulence with large eddies. Reichrath et al [12] conducted CFD simulations in order to validate the pressure distributions on the roof of both a 52 span and 7 span Venlo-type glasshouse. Each glasshouse simulation was conducted using both the standard $k-\epsilon$ turbulence model and the RNG turbulence model. They found acceptable agreement between the predictions and the experimental results. The airflow patterns and heat fluxes in a roof-ventilated multi-span greenhouse with insect proof screens were investigated experimentally by Shilo et al [3]. They concluded that under leeward ventilation, the ventilation rate increases linearly with velocity. Similarly to previous studies, it was shown that in leeward ventilation, air velocities at plant level is opposite to that of the external wind.

The work performed in this investigation focuses specifically on the parametric design of greenhouses, and will be validated by experimental work at a later stage.

COMPUTATIONAL FLUID DYNAMICS

Introduction

Computational Fluid Dynamics (CFD) is a research and design tool, which can produce quantitative predictions of fluid flow. These predictions are based on the laws of conservation (mass, momentum and energy) [13]. Although computational fluid dynamics yields only approximate solutions, it has a number of advantages. The results can be produced at a relatively low cost and quickly. The solutions may provide detailed information about the variables throughout the flow field. It is also relatively simple to change the parameters of the domain of interest. CFD also enables the user to simulate both realistic and ideal conditions [13].

The commercial CFD package StarCCM+ [14] was used to investigate the indoor climate of the greenhouses in this study numerically. The software is based on the finite volume method. This method subdivides the solution domain into a finite number of small control volumes, which correspond to the cells of a computational grid. Discrete versions of the integral form of the continuum transport equations are applied to each volume. The objective of this method is to obtain a set of linear algebraic equations to solve. An algebraic multigrid solver is then used to solve the resulting linear equations. To illustrate this, the transport of

a simple scalar will be considered. The continuous integral form of the governing equation is typically given by Eq. (1), [14]:

$$\frac{d}{dt} \int_V \rho \phi dV + \oint_A \rho \phi (\mathbf{v} - \mathbf{v}_g) \cdot d\mathbf{a} = \oint_A \Gamma \phi \cdot d\mathbf{a} + \int_V S_\phi dV \quad (1)$$

The four terms in the above equation are the transient term, the convective flux, the diffuse flux and the volumetric source term respectively. The transient term is generally only included where time effects become dominant. Each term is formulated mathematically in the StarCCM+ documentation [14], as well as in for instance Versteeg et al [15]. If the continuous integral form of the governing equation is discretized, Eq. (2) is obtained:

$$\frac{d}{dt} (\rho \phi V)_0 + \sum_f [\rho \phi (\bar{\mathbf{v}} \cdot \bar{\mathbf{a}} - G)]_f = \sum_f (\Gamma \nabla \phi \cdot \bar{\mathbf{a}})_f + (S_\phi V)_0 \quad (2)$$

The discretization procedure is described in some detail by Patankar [16] and Versteeg [15]. In order to model natural convection, the buoyancy source terms are included in the momentum equation by activating the gravity model. By selecting the constant density flow option, the buoyancy source term can be approximated by implementing the Boussinesq model as shown below in Eq. (3):

$$f_g = \rho \bar{g} \beta (T_{ref} - T) \quad (3)$$

StarCCM+ contains two models to model flow and energy, namely the segregated and coupled flow models. In order to solve the conservation equations for mass, momentum and energy simultaneously using a time or pseudo-time marching approach, the coupled flow model was chosen as well as an extension of this model, the coupled energy equation. The formulation used by this model is particularly robust for solving flows with dominant source terms such as buoyancy. [14] The turbulent nature of inner and outer flows in greenhouses was already indicated by previous investigations [17] In StarCCM+ turbulence is also simulated by solving the Reynolds-averaged governing equations for momentum, energy and scalar transport. Various turbulence models are available in StarCCM+; for this investigation the standard $k-\epsilon$ model was implemented. This model is a two-equation model in which transport equations are solved for the turbulent kinetic energy k and its dissipation rate ϵ . The transport equations used are in the form suggested by Jones and Launder [18]. Additional terms have been added in StarCCM+ to account for buoyancy (in this case the Boussinesq approximation) and compressibility effects although compressibility is not considered in this paper.

Numerical Greenhouse Models

The initial greenhouse, which was based on a study found in the literature [7] was already validated previously. [10] This greenhouse contained four spans (width, 4 by 9.60m; length, 68m; eaves height, 3.90m; ridge height, 5.9m) and was covered by 4mm thick horticulture glass. The greenhouse roof was equipped with continuous roof vents on both sides

of each span. In this simulation, the roof vents were opened toward the leeward side. During the experimental period, ornamental 0.2m high plants were grown on 0.75m shelves, but since they were small plants with a low transpiration rate, their presence was ignored in the numerical analysis. The length of the shelves were assumed, and the ventilator openings were assumed to be 1.22m wide [2]. A plastic partition separated the first two spans of the greenhouse.

The negative y direction was chosen as the direction of the gravitational constant for the further greenhouse models shown in this paper. The models considered consisted of the previous four span greenhouse for comparison purposes with further spans added on to study their effect on the flow situation upstream as well as downstream. For the sake of clarity no shelves were modelled in any downstream greenhouse or greenhouse span. The wind was modelled to act in an eastern direction at 1m/s. Figure 1 shows both the meshes for the first case (with the second greenhouse placed on the leeward side) and the second case (additional four spans attached to original four span greenhouse)

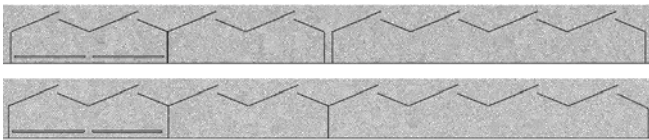


Figure 1: Two Separate Greenhouses and an Eight Span Greenhouse

A large control volume (334m×160m) was created around the greenhouses in order to minimize interference with the flow inside the greenhouse and to allow for development and definition of the boundary layer. Similar boundary conditions to the initial investigation [10] were applied to the domain boundaries in the numerical model. Before the final mesh was created, the mesh around the greenhouse was refined to a brick-shaped volume shape with a relative size of 6% of the chosen base size. The domain was meshed using a polyhedral meshing model, together with a boundary layer meshing model. The prism layer model was activated to ensure adequate modelling of the flow in the boundary layer. The prism layer mesh consisted of 5 orthogonal prismatic cells, with a combined thickness of 0.01m. The prism layer was present on all the wall-type boundaries in the solution domain. A tetrahedral mesh was created initially, after which a special dualization scheme was implemented to generate the polyhedral mesh, which consists of arbitrary shaped polyhedral cells. Once the three-dimensional mesh was created, the mesh was converted to a two-dimensional mesh to reduce running time. [7] Monitor points were inserted at various points to examine the progress of the solution. A line probe was inserted at 1m level to obtain the velocity and temperature distribution at plant level.

As an initial solution, steady, laminar conditions were assumed, after which the turbulence model was activated. The results indicated poor convergence, as well as an inherently transient flow. Lastly, the coupled solver was activated together with gravity and the implicit unsteady solver used in StarCCM+ [14].

Boundary Conditions

Both the inlet and outlet boundaries were specified as velocity inlet boundaries, but the outlet velocity was specified in the negative x-direction. This is not a true reflection of the real situation but the boundaries are so far removed from the greenhouse that this is assumed to be reasonable for the current purpose. The top boundary of the control volume was specified as a wall boundary, with a tangential velocity of 1 m/s in the x-direction. Table 1 summarizes the temperatures used for the wall boundaries of the greenhouse in the model. After obtaining the first set of results, additional spans were added to the initial greenhouse, shown in Figure 3. The three cases investigated are:

Case1: Two Separate Greenhouses with a distance of 1m in between

Case 2: An Eight Span Greenhouse

Case3: Two Separate Greenhouses with a distance of 2m in between the greenhouses.

Table 1: Boundary Conditions used in CFD Model Similar to Ould Khaoua [7]

PARAMETERS	VALUES
Inlet Air	
Velocity at 6m [m/s]	1.4
Temperature [°C]	22.2
Temperature [°C]	
Outside Air	22.2
Outside Ground	27.9
Inside Ground	27.3
Roof	33.6
Plastic Central Partition	31.3
Glass Walls	29.1

RESULTS

In order to investigate the efficiency of the leeward opened vents, the velocity and temperature differences at plant level are compared. The velocity magnitudes and air temperature for Case 1 (Additional Greenhouse on the leeward side) are compared to Case 2 (Additional 4 Spans attached to the original greenhouse). The temperature and velocity scalar plots for the two cases are shown in Figure 2 and 3 respectively.

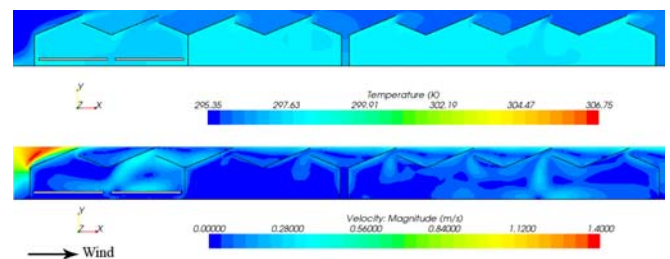


Figure 2: Temperature (K) and Velocity Plot (m/s) (Two Separate Greenhouses)

For the first case, the main stream of air moves into the greenhouse through the second roof vent, creating a strong anti-clockwise convective loop. Part of this air stream splits near the second shelf, moves back along the first shelf,

upwards against the glass and out the first roof vent. There is also air movement underneath the shelves, moving in opposite directions. Air is also sucked in at the fourth roof vent, which splits up into an anticlockwise convective loop against the glass wall, and a weaker clockwise loop, forcing some of the air out of the fourth roof vent as well. Most of the flow falls to the floor, and moves toward the plastic partition, where it exits at the third roof vent.

In the second separate greenhouse, air moves both in and out the first roof vent, as the inflow immediately forms two opposite rotating loops, and the loop closest to the glass wall forces the air out again. Similar conditions prevail at both the second and third roof vents, where the incoming air streams splits into two opposite rotating cells, forcing some air out the same vent. The air entering through the third vent actually falls all the way to the floor before it splits up, whereas the air entering at the second vent enters more diagonally, forming smaller convective loops as well. All the air that splits from the third roof vent towards the glass wall moves along the floor and up the glass wall, where it finally exits at the fourth roof vent.

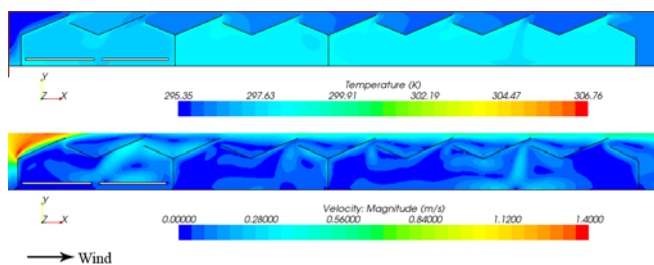


Figure 3: Temperature (K) and Velocity Plot (m/s) (Eight Span Greenhouse)

In the eight span greenhouse, air moves in at the second roof vent and forms an anti-clockwise convective loop above the second shelf. Part of the flow entering at the second roof vent splits and moves toward the first span where small loops are formed, and the flow exits at the first roof vent, joining the flow on the roof. Air is also entering at the fourth roof vent, forming a weaker anti-clockwise loop. Most of the flow moves along the floor towards the third span, up against the plastic partition, and out at the third roof vent. Three smaller convective loops are formed in the third span. The strongest cell is formed right beneath the seventh roof vent, where air is sucked in, and splits into two separate streams. Two convective loops are formed on each side of this air stream. Most of the flow moves along the floor towards the fifth span containing a partition, and exits at both the fifth and sixth roof vents. Due to smaller convective loops next to the roof vents below the roof, some air is also sucked back in. The rest of the flow entering at the seventh roof vent moves along the floor and upwards against the glass wall, and exits the greenhouse at the eighth roof vent.

Comparison of First Four Spans

In the next section, the first four spans and last four spans for the first two cases are compared respectively in Figures 4,5,6 and 7. Figure 4 graph indicates that the velocity increases towards the second span in both cases and that the

maximum velocity is reached at a similar location for both cases in the first two spans, although it is slightly lower for the second case. The velocity in the first span is overall slightly lower for the case of the eight span greenhouse. In the last two spans, the velocity distribution is more homogeneous compared to the first two spans, and in this case, the velocity for the first case containing the second separate greenhouse is somewhat lower. Figure 5 illustrates a relatively homogeneous temperature distribution for all four spans. In the first two spans, Case 1 exhibits a slight increase in temperature compared to Case 2. But the opposite is true for the last two spans, where Case 1 has a slightly lower temperature for the spans compared to Case 2.

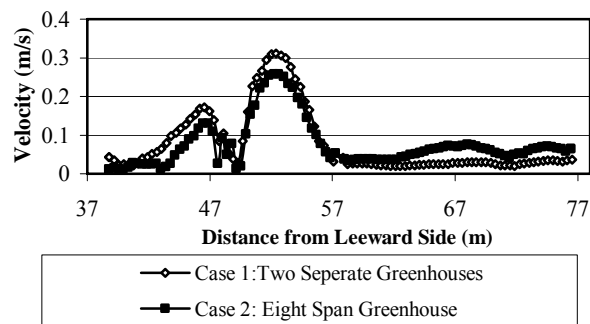


Figure 4: Comparison of Velocity Magnitudes at Plant Level for the First Four Spans (Case 1 & 2)

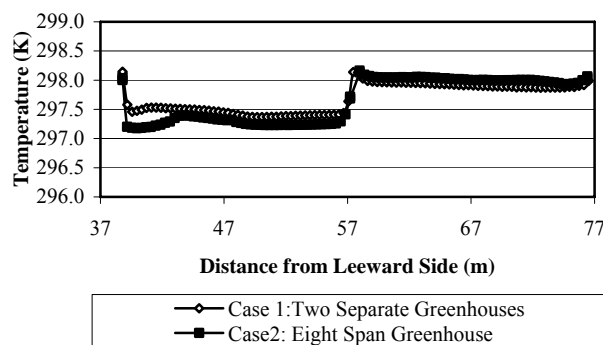


Figure 5: Comparison of Temperature Distribution at plant level for the First Four Spans (Case 1 and 2)

Comparison of Last Four Spans

Figure 6 page compares the velocity magnitudes at plant level for the last spans of both cases. The figure indicates that the velocity distribution is quite heterogeneous for both cases, varying from as low as almost 0 m/s to a maximum of approximately 0.17m/s. The maximum velocity for the eight span greenhouse shifts slightly towards the left. An intermediate peak velocity of approximately 0.1m/s occurs in the sixth span for Case 1. The temperature distribution at plant level, seen in Figure 7, contrary to the velocity, is relatively more homogeneous. Temperatures vary from approximately 298.3K down to 297.7K. Roughly the same trend however is exhibited by the velocity and temperature distributions for both cases.

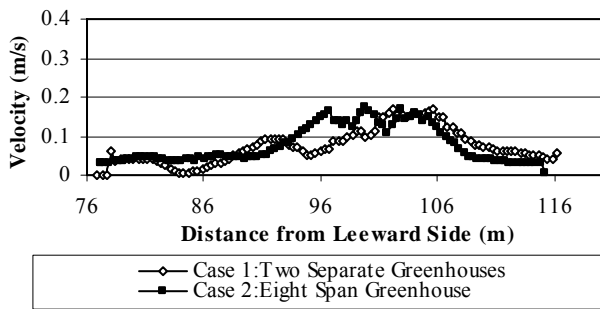


Figure 6: Comparison of the Velocity Magnitudes at Plant Level for the Last Four Spans (Case 1 & 2)

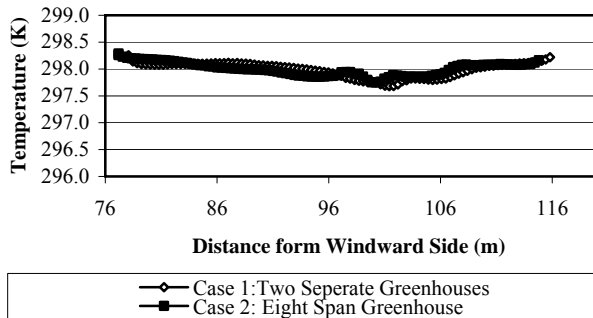


Figure 7: Comparison of the Temperatures at Plant Level for the Last Four Spans (Case 1 & 2)

Case 3: 2m Distance between Separate Greenhouses

In order to perform computational parametric studies, the control volume length behind the greenhouses was decreased slightly to reduce the running time. Figure 8 compares the velocity magnitudes of a full length greenhouse control volume to the reduced one over the first four spans.

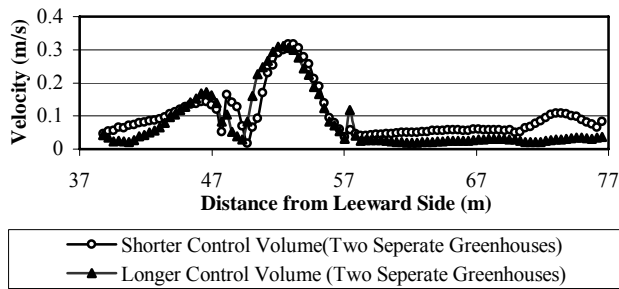


Figure 8: Comparison of Velocity Magnitudes for Different Control Volumes

The comparison seen in Figure 8 indicates that the difference in velocity magnitudes from the two different numerical models for case 3 is not too drastic. This model was then used to perform a parametric design study, adding once again an additional greenhouse, now at a distance of 2m from the first greenhouse (Case 3). The velocity magnitudes and temperatures in the first four spans are compared in Figures 9 and 10 respectively.

Comparison of the First Four Spans

Figure 9 shows that by moving the second greenhouse to a distance of 2m from the first greenhouse the climate inside the greenhouse is influenced to a small extent.

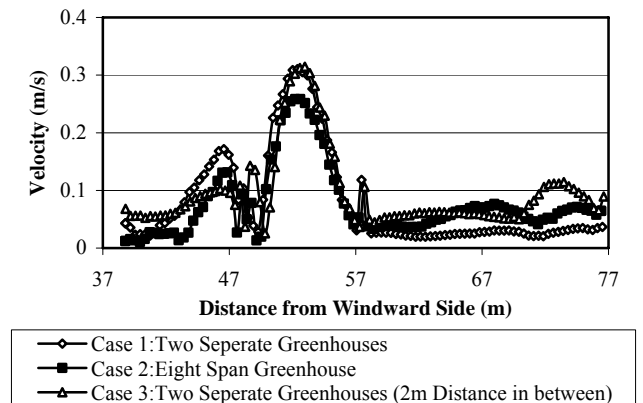


Figure 9: Comparison of Velocity Magnitudes for the First Four Spans (Case 1, 2 and 3)

The velocity increases from the first span, reaching a maximum in the second span. The maximum velocity for this case is comparable to the maximum obtained for case 1, although the velocity is slightly less in the first span. The velocity in the last two spans increases slightly toward the glass wall in the fourth span for Case 3.

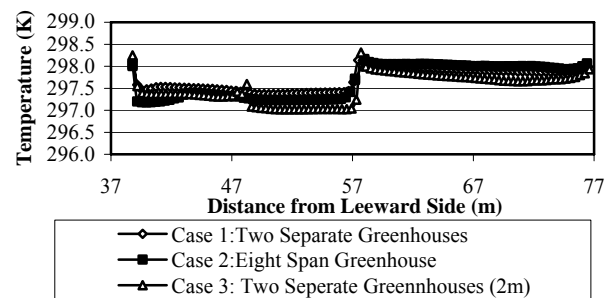


Figure 10: Comparison of Temperatures for the First Four Spans (Case 1, 2 and 3)

Figure 10 indicates that if the second greenhouse is moved 2m towards the leeward side, the temperature distribution within the first four spans are still relatively homogeneous, as well as somewhat lower compared to the first two cases.

Comparison of the Last Four Spans

Figures 11 and 12 shows the numerical velocity magnitudes and temperatures obtained for the last four spans for all three cases. Figure 11 illustrates that the velocity distribution in the last four spans are still relatively heterogeneous, with a small increase in the sixth and seventh spans. Figure 11 illustrates the velocity for Case 3 also heterogeneous throughout the last four spans, and also slightly different, especially in spans five and six. The maximum velocity is approximately 0.16 m/s, occurring at a similar position as the other two cases, with a comparable magnitude. The velocity decreases toward the rear of the last span. Figure 12 indicates the temperature is not significantly influenced by

the increased distance between the greenhouses, and is increased only to a small extent in the last four spans.

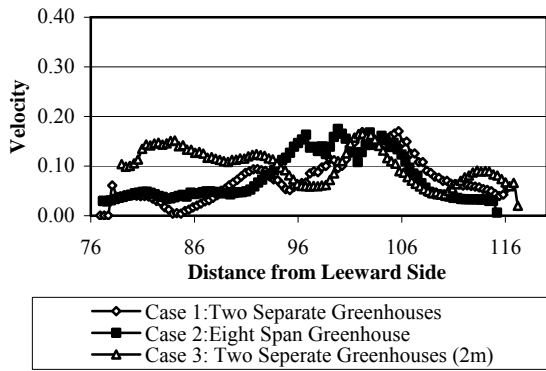


Figure 11: Comparison of Velocity Magnitudes for the Last Four Spans (Case 1, 2 and 3)

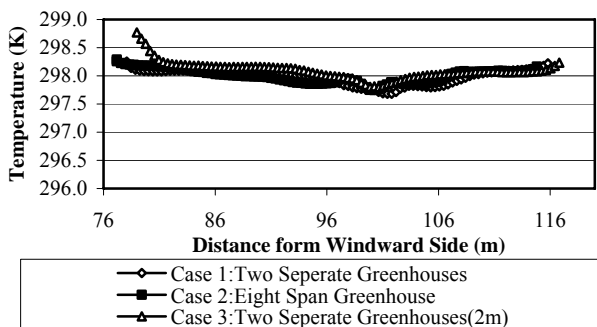


Figure 12: Comparison of Temperatures for the Last Four Spans (Case 1, 2 and 3)

Comparison to Original Four Span Greenhouse

Figures 13 and 14 display a comparison of the velocity and temperatures of case 2 compared to the original four span greenhouse [10]. This is shown to validate and compare the current results in some sense in the absence of real current experimental data. Both these graphs suggest that by adding another four spans to the original four span greenhouse the indoor climate specifically in the first four spans is influenced to a small extent. A 6% approximate change in velocity magnitude can be calculated.

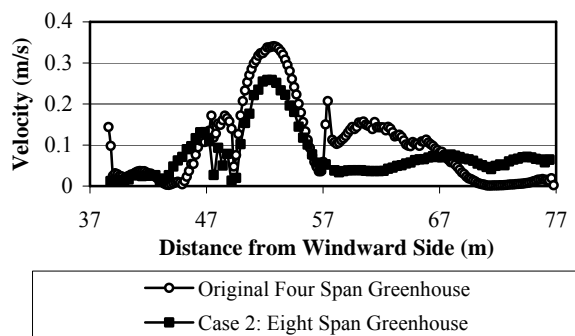


Figure 13: Comparison of Velocity Magnitude (Case 2) with Original Four Span Greenhouse (First Four Spans)

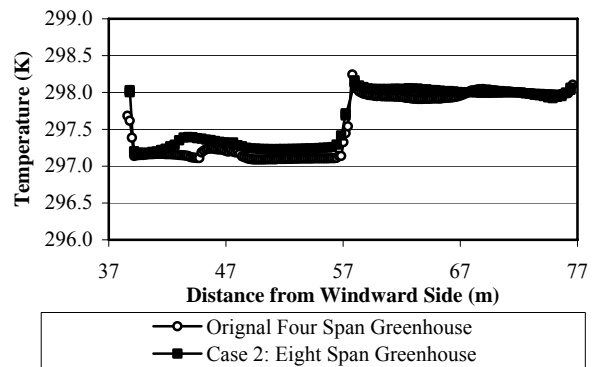


Figure 14: Comparison of Temperature Magnitude (Case 2) with Original Four Span Greenhouse (First Four Spans)

The purpose of this paper was to investigate the indoor climate in single and multi-span greenhouses. A possible topic for further investigation would be to investigate the presence of internal partitions on the indoor climate of the greenhouse. An indication of this has already been evaluated to some extent for a single four span greenhouse, containing a plastic partition in the centre, as well as a partition with a height half of that of the full height of the greenhouse. Figure 15 displays the contour plot for this scenario. This gives a reasonable indication of the influence of the partition.

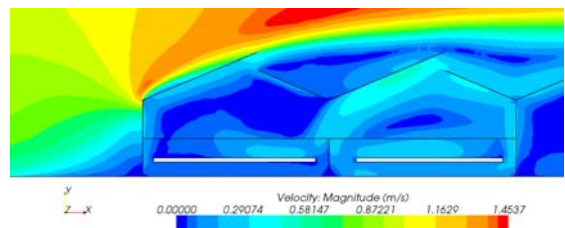


Figure 15: Velocity Contour Plot in First Two Spans Containing a half-partition

This contour plot indicates a heterogeneous velocity distribution in the first two spans, with a large convective cell appearing in the second span. The maximum velocity reached in the second span is also slightly higher compared to the first span taken at plant level.

CONCLUSION

In this study, a two-dimensional computational fluid dynamics model was developed and used to investigate the indoor climate of separate greenhouses compared to multi-span greenhouses. A parametric study was also conducted by moving the second greenhouse leeward as to create a space of 2m between the two greenhouses. From the scalar and vector plots, the dynamics of the air entering and leaving the greenhouse are somewhat different if the first two cases are compared. If all the graphs illustrating the numerical velocity and temperature distribution are evaluated, it can be concluded that for this specific type of greenhouse, adding another four spans, whether they are attached or separate, only influences the indoor climate to some extent. A more pronounced difference in the velocity distribution becomes evident once the distance between the greenhouses is increased. The results indicate that there is a

notable difference between the indoor climate in the first four spans compared to the last four spans. This may influence crop growth in the two different sections. This result however cannot be generalised since it is specific to the geometry of the greenhouse under investigation. Further research into the distance between the greenhouses is required specifically in the case where side ventilators are present. The influence of partitions inside the greenhouse should also be investigated. Furthermore the effect of the prism layer characteristics should also be addressed in more detail to determine the effect of the boundary log-law models used. The effect of change in inlet turbulence may also be addressed. More research into detailed flow patterns in downstream greenhouses with internal shelves and partitions may also be done as it represents a downstream effect.

REFERENCES

1. American Society of Heating, Refrigeration and Air-conditioning Engineers, (2001) 2003 *ASHRAE HVAC Applications SI Edition*, ASHRAE, Atlanta
2. Boodley J.W. (1981) *The Commercial Greenhouse*, New York: Delmar Publishers
3. Shilo E., Teitel M., Mahrer Y., Boulard T., Air-flow patterns and heat fluxes in roof-ventilated multi-span greenhouse with insect-proof screens, *Agricultural and Forest Meteorology* (2004) 122, 3-20
4. Norton T., Sun D. Grant J., Fallon R., Dodd V., Applications of Computational Fluid Dynamics (CFD) in the modelling and design of Ventilation Systems in the Agricultural Industry: A Review, *Bioresource Technology* 98 (2007) 2386-2414
5. Mistriotis A. Bot G.P.A., Picuno P., Scarascia-Mugnozza G., Analysis of the efficiency of greenhouse ventilation using computational fluid dynamics., *Agricultural and Forest Meteorology* 85 (1997) 217 - 228
6. Bartzanas T., Boulard T., Kittas C., Effect of Vent Arrangement on Windward Ventilation of a Tunnel Greenhouse, *Biosystems Engineering* (2004) 88 (4) 479-490
7. Ould Khaoua, S.A., Bournet,P.E., Migeon,C., Boulard T.,Chassériaux. (2006), Analysis of greenhouse Ventilation Efficiency based on Computational Fluid Dynamics, *Biosystems Engineering* (2006) 95 (1) 83-98
8. Bournet P.E., Ould Khaoua S.A., Boulard T., Numerical prediction of the effect of vent arrangements on the ventilation and energy transfer in a multi-span glasshouse using a bi-band radiation model., *Biosystems Engineering* (2007) Volume 98, Issue 2, Pages 224-234
9. Kruger S., Pretorius L., The Effect Of Ventilator Configurations In Naturally Ventilated Greenhouse Applications., *Proceedings of the 10th UK National Heat Transfer Conference, 2007*, Edinburgh, Scotland
10. Kruger S., Pretorius L., 2007, The Effect of Internal Obstructions in Naturally Ventilated Greenhouse Applications, *Proceedings of the 5th International Conference on Heat Transfer, Fluid Mechanics and Thermodynamics 2007*, Sun City, South Africa
11. Wang S., Deltour J., Lee-side Ventilation-induced Air Movement in a Large-scale Multi-span Greenhouse. *Journal of Agricultural Engineering Research* (1999) 74, 103-110
12. Reichrath S., Davies T.W., Computational Fluid Dynamics Simulations and validation of the Pressure Distribution on the roof of a Commercial Multi-span Venlo-type Greenhouse, *Journal of Wind Engineering and Industrial Aerodynamics* (2002) 90, 139-149
13. Kundu P.K., Cohen I.M., 2004, *Fluid Mechanics*, 3rd Edition, Elsevier Academic Press, California USA
14. StarCCM+ (2006) CFD Manuals, CD-Adapco
15. Versteeg, H.K., and Malalasekera W., 2007 *An introduction to Computational Fluid Dynamics, The Finite Volume Method*, 2nd ed., Pearson Prentice Hall, England.
16. Patankar S.V. ,1980, *Numerical Heat Transfer and Fluid Flow*. Washington: Hemisphere
17. Boulard T., Wang S., Haxaire R. ,2000, Mean and Turbulent air flows and microclimatic patterns in an empty greenhouse tunnel. *Agricultural and Forest Meteorology*, 100, pp 169 - 181
18. Jones W.P., Launder B.E., 1971, The prediction of Laminarization with a Two-Equation Model of Turbulence, *International Journal of Heat and Mass Transfer* Vol. 15 pp 301 - 314